

Electrospray on superhydrophobic nozzles treated with argon and oxygen plasma

Doyoung Byun,^{1,a)} Youngjong Lee,¹ Si Bui Quang Tran,¹ Vu Dat Nguyen,¹ Sanghoon Kim,² Baeho Park,² Sukhan Lee,³ Niraj Inamdar,⁴ and Haim H. Bau⁴

¹Department of Aerospace Information Engineering, Konkuk University, Republic of Korea

²Department of Physics, Konkuk University, Republic of Korea

³School of Information and Communication Engineering, Sungkyunkwan University, Republic of Korea

⁴Department of Mechanical Engineering and Applied Mechanics, University of Pennsylvania, Pennsylvania 19104, USA

(Received 27 November 2007; accepted 14 January 2008; published online 7 March 2008)

We report on a simple process to fabricate electrohydrodynamic spraying devices with superhydrophobic nozzles. These devices are useful, among other things, in mass spectrometry and printing technology. The superhydrophobic nozzle is created by roughening the surface of the polyfluorotetraethylene (PTFE) by argon and oxygen plasma treatment. We have developed a polymer-based electrospray device with a flat, superhydrophobic nozzle capable of maintaining a high contact angle and stable jetting. © 2008 American Institute of Physics.

[DOI: 10.1063/1.2840725]

Electrohydrodynamic spraying, or electrospray, allows for the dispersal of very fine liquid droplets. This technology has numerous potential applications including mass spectrometry,^{1–3} printing technology,^{4–6} and biological microarrays.⁷ Briefly, when liquid is pumped through a capillary and subjected to an electric field, an electric charge is induced on the meniscus. The combination of electrostatic, hydrostatic, and capillary forces elongate the liquid into a conical shape known as the Taylor-cone.^{8–10} Depending on the flow rate of the liquid and the applied electric field's intensity, the cones may either emit drops or fine jets (the “cone-jet” mode) that subsequently break into fine droplets. The cone-jet spraying mode, in which a steady jet of charged droplets is emitted from the apex of the Taylor cone, allows one to spray drops in the submicron range.¹⁰

Nanodispensing electrospray has been used for the nanoliter transport of biomaterials. Kuil *et al.*¹¹ developed a computer-controlled method to deposit on a substrate arrays of nanoliter drops laden with proteins. Electrosprays are also often used in mass spectroscopic analysis of biomolecules.^{1–3,12}

More recently, there has been increasing interest in direct writing and inkjet printing on the micro level due to their low cost and rapid deposition.^{13,14} de Gans *et al.*¹³ anticipate using inkjet printing to form circuits and other electronic components from conductive polymers.¹¹

Conventional inkjet devices, based on thermal bubbles or piezoelectric pumping, suffer from fundamental limitations, such as relatively large size and low density of the nozzle array. In contrast, electrohydrodynamic jet printing^{4,6} and electrostatic field induced jetting devices,⁵ which are based on the direct manipulation of liquids by electric fields, can be made smaller and can operate at higher frequencies. For example, Lee *et al.*⁵ have developed an electrostatic field induced inkjet head for drop-on-demand jetting operation. Their design is able to provide relatively stable and sustainable droplet ejection. However, in many industrial applications, one needs multinozzle devices which can be manufac-

tured massively and produced with appropriate yield.

Hence, we developed jetting nozzles that can be readily extended to multinozzle devices as well as mass production. Polymer based fabrication is one attractive approach for large scale production of devices by means of injection molding or drilling. Figure 1 presents schematics and photographs of polymer-based electrospray devices. Figures 1(a)

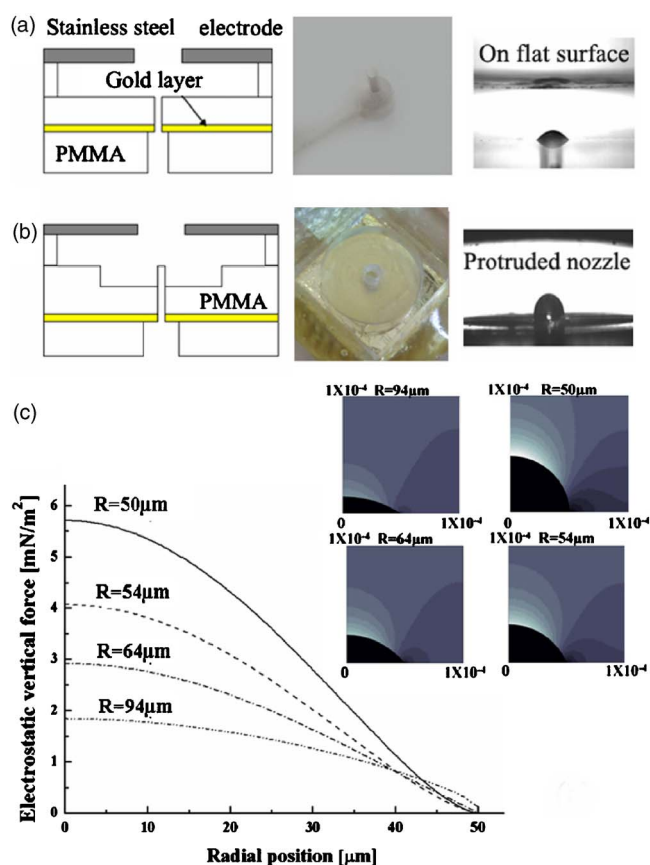


FIG. 1. (Color online) A schematic (left) and a photograph (middle) of the polymer-based electrospray device and a meniscus at the tip of nozzle (right). (a) Flat nozzle and (b) Protruding nozzle. (c) Electrostatic field (inset) and the electrostatic force at the cone's surface when the drop diameter is $R=50, 54, 64$, and $94 \mu\text{m}$.

^{a)} Author to whom correspondence should be addressed. Electronic mail: dybyun@konkuk.ac.kr. Tel.: +82-2-450-4195. FAX: +82-2-444-6670.

and 1(b) depict, respectively, a device with a flat nozzle [the nozzle is simply a circular hole in the surface of the polymethyl methacrylate (PMMA)] and a device with a protruding nozzle. The protruding nozzle can improve the meniscus shape by preventing the drop from spreading along the flat surface. Beneath the nozzle's surface, we deposit a 200 Å thick layer of gold to form the driving electrode. Above the device, there is a ring-shaped stainless steel electrode that serves as the ground. The liquid reservoir is made from PMMA and the devices are manufactured by using conventional machining technology.

Figure 1 shows the difference between the liquid menisci formed on the flat [Fig. 1(a)] and the protruding [Fig. 1(b)] nozzles. Witness that the drop formed on the protruding nozzle has a larger apparent contact angle than the drop that forms on the flat nozzle. The jetting phenomena was observed through the polymer based nozzle, which is a dielectric material with similar properties to the glass capillary nozzles.^{4,5} Both the flat and protruding nozzles concentrated the electric field at the apex of the liquid meniscus. Even though both the flat and protruding nozzles ejected liquid, the higher contact angle of the protruding nozzle allowed us to more easily generate a cone jet and sustain its stability during the jetting process.

To examine the effects of the meniscus shape on the electrostatic force, we numerically solve the Maxwell equation for the electric field and the electrostatic force¹⁵ using the finite element software COMSOL MULTIPHYSICS (Comsol Inc.).

We simulated an axisymmetric two-dimensional geometry to model the circular nozzle with the liquid meniscus at its tip [Fig. 1(a)]. In the simulation, the distance between the nozzle and the top electrode is 200 μm , the nozzle diameter is 50 μm , and the applied voltage is 200 V. The shape of the meniscus is determined by specifying the curvature (R) of the meniscus. Figure 1(c) depicts the vertical component of the electrostatic force as a function of the radial position. Witness that the electric field's strength near the apex of the meniscus increases as the contact angle increases (the drop's curvature decreases). Thus, it is desirable to increase the contact angle.

One can increase the contact angle through the use of hydrophobic surfaces.¹⁶ However, even on a hydrophobic surface with a contact angle of around 110°, the cone jet generated by a flat nozzle is not stable and the meniscus on top of the nozzle may overflow onto the surrounding surface. One can eliminate these instabilities by fabricating protruding nozzles. Unfortunately, the protruding nozzle is difficult to manufacture. A flat nozzle, composed of a superhydrophobic surface (with a static contact angle greater than 150°)¹⁷ is most advantageous as the high-contact angle of the liquid meniscus at the nozzle's opening diminishes potentially hazardous spreading of the liquid and ensures long term stability and repeatability of the electrospray process.

A known process for creating a superhydrophobic surface is ion beam treatment.¹⁸ Capps *et al.*¹⁹ reported on the effectiveness of argon and argon-oxygen ion beams in modifying the topology and wetting characteristics of polymer surfaces, in particular, polyfluorotetraethylene (PTFE).

In order to create a superhydrophobic nozzle, we use argon and oxygen ion beams to treat the PTFE surface. The contact angle of a droplet of de-ionized (DI) water was measured with a charge coupled device camera. Figure 2(a) de-

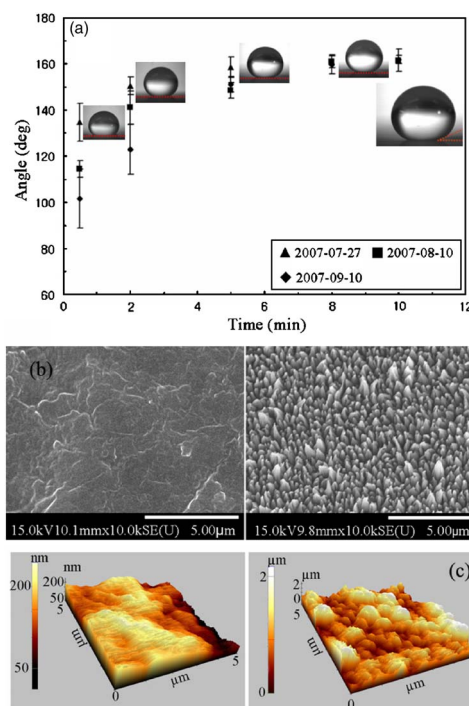


FIG. 2. (Color online) Superhydrophobic surface. (a) The contact angle of a PTFE polymer surface treated by an argon (2 SCCM) and oxygen (2 SCCM) plasma ion beam at 1.5 keV. The contact angle was measured immediately after treatment (triangles), one month later (squares), and two months later (diamonds). (b) SEM images of untreated (left) and treated (right) PTFE surfaces. (c) AFM images of untreated (left) and treated (right) PTFE surfaces.

picts the contact angles of the liquid meniscus as a function of the surface's exposure time to the ion beam immediately after exposure (triangles), one month (squares), and two months after exposure (diamonds). The flow rate of argon and oxygen gas was 2 SCCM (SCCM denotes cubic centimeter per minute at STP), and the energy source of the ion beam was 1.5 keV. As the exposure time increased so did the contact angle until it reached an asymptotic value after about 8 min exposure. The surface exposed to the beam for just a short time exhibited significant aging. When we exposed the PTFE to the ion beam for 10 min, we were able to sustain contact angles greater than 160° for two months.

Figure 2(b) shows the morphology of the raw and treated PTFE surfaces taken with a scanning electron microscope (SEM). The left image is the untreated PTFE surface, while the right image is the treated PTFE surface. The raw PTFE surface is quite smooth compared to the treated PTFE sur-

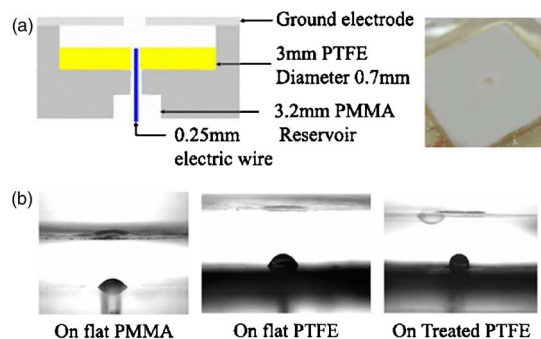


FIG. 3. (Color online) Electrospray device. (a) A schematic and a picture of the superhydrophobic nozzle treated by a plasma ion beam. (b) Comparisons of the menisci on top of nozzles in flat PMMA, flat untreated PTFE, and treated PTFE surfaces.

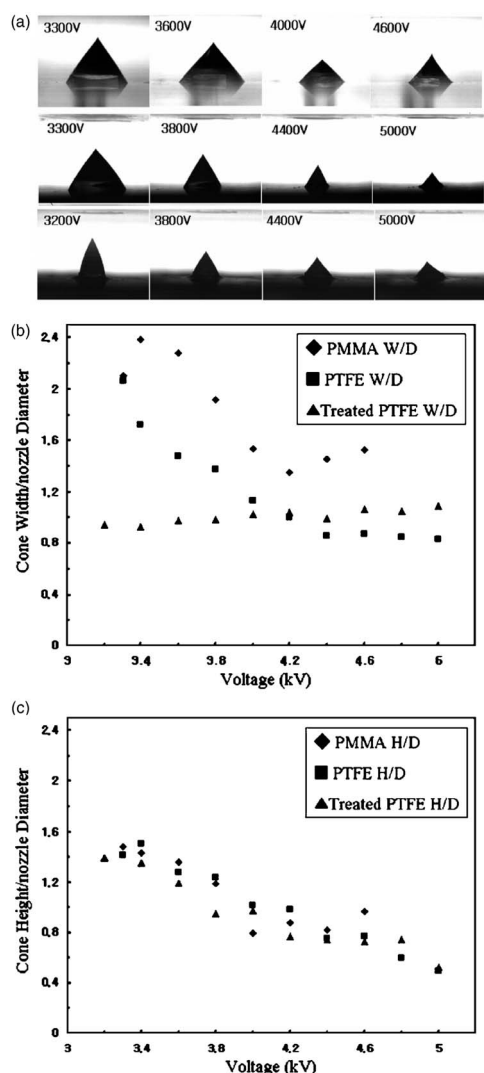


FIG. 4. Electro spray emitted by various nozzles. (a) Jetting images through nozzles on flat PMMA, untreated flat PTFE, and treated PTFE surfaces as functions of applied voltage. (b) The cone's diameter (normalized with the nozzle's diameter) as a function of applied voltage. (c) The cone's height as a function of applied voltage.

face, which exhibited nanoscale structures due to the high energy ion bombardment. To measure the nanostructure quantitatively, we scanned the untreated and treated PTFE surfaces using an atomic force microscope (AFM), as shown in Fig. 2(c). The width and height of the nanoscale structures of the treated surface are ~ 200 nm and 1.2 μm , respectively. It is due to these nanoscale structures that we can increase the liquid meniscus contact angles to the superhydrophobic range.

Figure 3(a) depicts schematically the electro spray device with a PTFE nozzle treated with Ar and oxygen ion plasma. The PTFE is treated by the ion beam prior to integration with the PMMA reservoir.

From left to right, Fig. 3(b) shows the liquid drop on a flat PMMA, untreated PTFE, and treated PTFE surfaces. On the PMMA alone, we observe a small contact angle. The contact angle is higher on the untreated PTFE surface and still higher on the treated PTFE surface—similar to that on the protruding nozzle. The treated PTFE nozzle ensures long term stability and repeatability of the electro spray process.

Figure 4(a) shows jetting images through three flat nozzles of diameter 300 μm at various applied potentials. The top, middle, and bottom rows correspond, respectively, to PMMA, raw (untreated) PTFE, and treated PTFE surfaces. Figures 4(b) and 4(c) depict, respectively, the diameter and height of the cones normalized with the nozzle diameter as functions of the applied voltage for the three surfaces. In the cases of the PMMA and raw PTFE surfaces and low voltage (<4 kV), the diameter of the cone jet was greater than the nozzle's diameter, which means undesirable instability and contamination around nozzle. In the above two cases, the cone's diameter decreased as the voltage increased until achieving a value that was somewhat larger than the nozzle's diameter. In contrast, the treated PTFE surface not only exhibited high contact angles, but the cone-jet diameter was equal to the nozzle's diameter. When the liquid meniscus does not overflow on the surface, the voltage does not affect the cone's diameter. Hence, we expect the treated nozzle to exhibit a stable and repeatable performance. In all cases, as the voltage increases, the electrostatic force, which extracts the liquid meniscus, strengthens and ejects more liquid, the ratio of cone height to nozzle diameter decreases [Fig. 4(c)].

To summarize, we have presented a polymer-based, electrostatic jetting or electro spray device with a flat, superhydrophobic nozzle capable of maintaining high contact angles and stable jetting.

This work was supported by a grant from the Korea Research Foundation (KRF-2003-D00032) and the National Research Laboratory Program, Korea Science and Engineering Foundation Grant (R0A-2007-000-20012-0). S.B.Q.T. and V.D.N. acknowledge partial support from the Korea Research Foundation (KRF-2005-D00208 and KRF-2007-211-D00019).

- ¹J. B. Fenn, M. Mann, C. K. Meng, S. K. Wong, and C. Whitehouse, *Science* **246**, 64 (1989).
- ²C. H. Yuan and J. Shiea, *Anal. Chem.* **73**, 1080 (2001).
- ³J. S. Kim and D. R. Knapp, *J. Am. Soc. Mass Spectrom.* **12**, 463 (2001).
- ⁴J. U. Park, M. Hardy, S. J. Kang, K. Barton, K. Adair, D. K. Mukhopadhyay, C. Y. Lee, M. S. Strano, A. G. Alleyne, J. G. Georgiadis, P. M. Ferreira, and J. A. Rogers, *Nat. Mater.* **6**, 782 (2007).
- ⁵S. Lee, D. Byun, D. Jung, J. Choi, Y. Kim, J. H. Yang, S. U. Son, S. B. Q. Tran, and H. S. Ko, *Sens. Actuators, A* **141**, 506 (2007).
- ⁶D. Y. Lee, Y. S. Shin, S. E. Park, T. U. Yu, and J. Hwang, *Appl. Phys. Lett.* **90**, 081905 (2007).
- ⁷M. D. Paine, M. S. Alexander, K. L. Smith, M. Wang, and J. P. W. Stark, *J. Aerosol Sci.* **38**, 315 (2007).
- ⁸J. Fernández de la Mora, *J. Fluid Mech.* **243**, 561 (1992).
- ⁹J. Fernández de la Mora, *Annu. Rev. Fluid Mech.* **39**, 217 (2007).
- ¹⁰M. Cloupeau and B. Prunet-Fuch, *J. Aerosol Sci.* **25**, 1021 (1994).
- ¹¹M. Kuil, J. P. Abrahams, and J. C. M. Marijnissen, *J. Biotechnol.* **1**, 969 (2006).
- ¹²B. Legrand, A. E. Ashcroft, L. Bucaillot, and S. Arscott, *J. Micromech. Microeng.* **12**, 509 (2007).
- ¹³B. J. de Gans, P. C. Duineveld, and U. S. Schubert, *Adv. Mater. (Weinheim, Ger.)* **16**, 203 (2004).
- ¹⁴R. A. Street, W. S. Wong, S. E. Ready, M. L. Chabiny, A. C. Arias, S. Limb, A. Salleo, and R. Lujan, *Mater. Today* **9**, 32 (2006).
- ¹⁵O. Lastowa, and W. Balachandran, *J. Electrostat.* **64**, 850 (2006).
- ¹⁶P. Lozano, M. Martínez-Sánchez, and J. M. Lopez-Urdiales, *J. Colloid Interface Sci.* **276**, 392 (2004).
- ¹⁷N. A. Patankar, *Langmuir* **20**, 8209 (2004).
- ¹⁸E. S. Yoon, S. H. Yang, H. S. Kong, and K. H. Kim, *Tribol. Lett.* **15**, 145 (2003).
- ¹⁹N. Capps, L. Lou, and M. Amann, See <http://www.advanced-energy.com/upload/File/Sources/SL-IONPOLY-260-01.pdf>.